

XMM-Newton Spectroscopy of the Galactic Microquasar GRS 1758–258 in the Peculiar Off/Soft State¹

J. M. Miller², R. Wijnands^{2,5}, P. M. Rodriguez-Pascual³,
P. Ferrando⁴, B. M. Gaensler^{2,6}, A. Goldwurm⁴, W. H. G. Lewin², D. Pooley²

Subject headings: Black hole physics – relativity – stars: binaries (GRS 1758–258) –
physical data and processes: accretion disks – X-rays: stars

ABSTRACT

We report on an *XMM-Newton* Reflection Grating Spectrometer observation of the black hole candidate and Galactic microquasar GRS 1758–258. The source entered a peculiar “off/soft” state in late February, 2001, in which the spectrum softened while the X-ray flux – and the inferred mass accretion rate – steadily decreased. We find no clear evidence for emission or absorption lines in the dispersed spectra, indicating that most of the observed soft flux is likely from an accretion disk and not from a cool plasma. The accretion disk strongly dominates the spectrum in this lower-luminosity state, and is only mildly recessed from the marginally stable orbit. These findings may be difficult to explain in terms of advection-dominated accretion flow, or “ADAF” models. We discuss these results within the context of ADAF models, simultaneous two-flow models, and observed correlations between hard X-ray flux and jet production.

1. Introduction

The source GRS 1758–258 was discovered with the *GRANAT*/SIGMA hard-X-ray/soft- γ -ray telescope (Sunyaev et al. 1991). It is often referred to as a “twin” source with 1E 1740.7–2942. Both are in the vicinity of the Galactic Center region, are strong emitters at hard-X-ray/soft- γ -ray energies, and display relativistic jets in the radio band (Mirabel et al. 1992; Rodriguez, Mirabel,

¹Based on observations made with *XMM-Newton*, an ESA science mission with instruments and contributions directly funded by ESA Member States and by NASA.

²Center for Space Research and Department of Physics, Massachusetts Institute of Technology, Cambridge, MA 02139–4307; jmm@space.mit.edu

³*XMM-Newton* SOC, Villafranca Satellite Tracking Station, PO box 50727, 28080, Madrid, Spain

⁴Service d’Astrophysique, DSM/DAPNIA, CEA/Saclay, F-91191 Gif sur Yvette, Cedex, France

⁵*Chandra Fellow*

⁶*Hubble Fellow*

& Marti 1992; Mirabel 1994). The hard spectrum of GRS 1758–258 extends to 300 keV and is similar to that of Cygnus X-1, and on that basis it is considered a black hole candidate (for a review of BHCs, see Tanaka & Lewin 1995).

The soft X-ray component in this source is usually very weak when the hard X-ray flux is at a typical strength. The soft component was too weak to be positively detected with *ASCA* (Mereghetti et al. 1997). However, a soft component below 2 keV, modeled with a power-law ($\Gamma_{\text{PL}} \sim 3$) was observed with *ROSAT* in 1993 when the hard power-law flux was less intense (Mereghetti et al. 1994). Similarly, the soft X-ray component was detected with *XMM-Newton* during a short, softer episode in September, 2000 (Goldwurm et al. 2001). In this observation, the soft component could be fit with a simple blackbody spectrum ($kT = 0.32$ keV).

In late February of 2001, observations with *RXTE* revealed a sharp drop in the hard (>10 keV) flux from GRS 1758–258, with no corresponding drop in the soft flux (Smith et al. 2001a,b,c). Smith et al. (2001c; hereafter, SHMS) report a steady decline in the 3–25 keV flux for 50 days following 27 February 2001. The soft component is clearly detected with the *RXTE*/PCA, and can be fit by both simple blackbody and multicolor disk (MCD; Mitsuda et al. 1984) blackbody models. This state is qualitatively similar to the “off” state observed by *GRANAT*/SIGMA between fall 1991 and spring 1992 (Gilfanov et al. 1993), during which the hard X-ray flux of GRS 1758–258 decayed beneath detection limits. We therefore refer to the present X-ray spectral state as the “off/soft” state.

We requested a *XMM-Newton* target of opportunity (TOO) observation of GRS 1758–258 for three principal reasons: to better understand the nature of the soft component, to understand the implications of the off/soft state for current accretion flow models, and to place the off/soft state within the context of emerging connections between spectral flux components and jets in BHCs (Fender et al. 2001). Herein we report the results obtained with the *XMM-Newton* Reflection Grating Spectrometer (RGS).

2. Observations and Data Analysis

Following our TOO request, GRS 1758–258 was observed for ~ 22 ksec starting at UT 09:48:12 on 22 March, 2001. RGS1 and RGS2 were operated in “spectral+Q” mode. The EPIC-MOS cameras were operated in “partial window, 100×100 ” mode, and the EPIC-PN camera in “large partial window, 200×384 ” mode. For the OM, “grism 1,” optimized for the ultraviolet band, was used.

Accurate analysis of bright sources like GRS 1758–258 requires a careful treatment of pile-up when dealing with the EPIC data. This in turn requires a good knowledge of the mirror response; the EPIC calibration team is developing a description of the in-flight calibration. The results presented in this work are therefore restricted to analysis of the RGS data, and results from the EPIC data analysis will be presented in future work. At the time of writing, the only previous

X-ray binary observations reported on with *XMM-Newton* are EXO 0748–676 (Bonnet-Bidaud et al. 2001; Cottam et al. 2001) and GRS 1758–258 (observation in September 2000, Goldwurm et al. 2001). Instrumental performance and systematic effects will become more clear as more sources with a strong soft continuum flux are observed.

We have used the spectral data and background files produced by the standard pipeline processing system at the *XMM-Newton* Survey Science Center (SSC) using Science Analysis Software (XMM-SAS) version 5.0. We estimate that fewer than 1% of the counts in the RGS spectra are from the nearby source GX 5–1.

To obtain improved statistical constraints on fitted models and to ensure the accuracy of Poisson statistics, we rebinned the background-subtracted first-order spectra from RGS1 and RGS2 by requiring a minimum of 20 counts per bin. After rebinning, between 0.35–0.60 keV the flux bin errors include zero. The flux bins steadily increase and the errors are inconsistent with zero above 0.60 keV. We therefore adopt 0.60 keV as the lower limit of our fitting range. Similarly, above 2.3 keV the flux bins have large errors and are consistent with zero, so we adopt 2.3 keV as the upper limit to our fitting range (the full energy range of the RGS is 0.35–2.50 keV).

Using XSPEC version 11.0 (Arnaud & Dorman, 2000), the RGS1 and RGS2 spectra are fitted simultaneously to account for any cross-calibration uncertainties. An overall normalization constant is allowed to float between the data obtained from each. Values obtained for this constant are approximately 0.95 for all fits.

3. Results

The results of our joint fits to the RGS spectra are detailed fully in Table 1. In each of the six models, the continuum components are multiplied by a model for photoelectric absorption (“wabs,” in XSPEC). Model 6 is a single-component model consisting of a simple power-law. Although statistically only marginally worse than models dominated by a thermal component ($\chi^2/\nu = 1.778, \nu = 1251$), the power-law index is abnormally high ($\Gamma_{\text{PL}} = 5.2 \pm 0.2$), and inconsistent with values obtained for other BHCs regardless of spectral state (for a review, see Tanaka & Lewin 1995). We therefore conclude that models dominated by a thermal component are required to fit the data from GRS 1758–258 in the off/soft state, and concentrate on these.

In models which include thermal and power-law components, the power-law index could not be constrained. In order to be consistent with models widely fit to BHCs, and especially those recently fit to GRS 1758–258, we fix the power-law indices in models 1–5 to those measured by SHMS via fits to *RXTE*/PCA data obtained on 12–13 March, 2001 in the 3–25 keV band using the same models. The fit results for models 1–5 indicate that the power-law component is not required in this energy range as a zero normalization is preferred. We quote 90% upper-limits for the 0.6–2.3 keV contribution from a power-law component in Table 1. In all cases, the power-law contributes less than 2% of the total flux in this band. This is consistent with *Chandra*

measurements in the 1–10 keV band during the off/soft state (Heindl and Smith 2001).

Models 1 and 3 consist of MCD and simple blackbody components, respectively, in combination with a power-law component ($\chi^2/\nu = 1.621$, $\chi^2/\nu = 1.587$, respectively, $\nu = 1252$). The data/model ratios obtained for models 1 and 3 are nearly identical (see Figure 1), and neither indicates the presence of any significant line emission (indeed, line emission is not indicated regardless of continuum model). In part, the poor χ^2 statistics obtained for these models (indeed, for all models) may be due to the approximately 5% normalization discrepancy between RGS1 and RGS2. A second contributing factor may be the relatively smaller RGS effective area above ~ 2 keV; we included this region after rebinning to better-constrain any power-law flux. When the characteristics of the RGS are more clearly known for strong continuum sources like GRS 1758–258, it may be possible to improve on the fits.

Models 2 and 4 are duplicates of models 1 and 3 respectively, except in models 2 and 4 we have fixed the neutral hydrogen column density (N_H) to 1.5×10^{22} atoms/cm² as per fits to *ASCA* data of GRS 1758–258 reported by Mereghetti et al. (1997). Model 5 is like 3 and 4 in that simple blackbody and power-law components are used to model the continuum, but in this model N_H is fixed to 1.74×10^{22} atoms/cm², as measured via fits to *XMM-Newton*/EPIC-MOS data on GRS 1758–258 obtained in September, 2000 (Goldwurm et al. 2001). There are no reasons to doubt the value of N_H we measure due to instrumental effects (e. g., CCD pile-up, as the RGS is a dispersive spectrometer). Rather, these models are fit to allow for comparisons to the results of SHMS and Goldwurm et al. (2001) as directly as possible.

Via the MCD model, SHMS obtain a color temperature of $kT = 0.464 \pm 0.007$ keV. Via model 1 (N_H free), we find a color temperature of $kT = 0.34 \pm 0.01$ keV. In both measurements, the errors are 90% confidence errors; these color temperatures are significantly different. Via model 2 (N_H fixed at SHMS value), we find a color temperature of $kT = 0.60 \pm 0.01$ keV. Again, this is significantly different from the value measured by SHMS. However, the fit with model 2 ($\chi^2/\nu = 2.227$, $\nu = 1251$) is statistically worse than that obtained via model 1 ($\chi^2/\nu = 1.621$, $\nu = 1252$).

SHMS report a simple blackbody temperature of $kT = 0.395 \pm 0.006$ keV. Fits with model 3 (N_H free) indicate $kT = 0.286 \pm 0.007$ keV, and via model 4 (N_H fixed at SHMS value) $kT = 0.378^{+0.005}_{-0.004}$ keV. The temperature measured via model 4 is only slightly lower than that measured by SHMS, and only marginally inconsistent at 90% confidence. However, the fit obtained with model 3 is statistically preferred and the temperature is significantly lower.

The blackbody temperature obtained via fitting with model 5, wherein N_H is fixed to the value measured by Goldwurm et al. (2001), is $kT = 0.332^{+0.002}_{-0.001}$ keV. They measure $kT = 0.32 \pm 0.02$ keV – these temperatures are consistent at 90% confidence. Statistically, model 3 is a marginally better fit, and for this model the measured temperature is significantly lower.

We attempted to describe the spectrum in terms of a diffuse plasma by fitting with the “mekal” and “raymond” models within XSPEC. Fits which are statistically only marginally worse

than those with models 1–6 are obtained, but only if the elemental abundances are allowed to assume values less than 0.2% of solar values. As this physical scenario is extremely unlikely, we do not further consider these models.

To test for the presence of narrow emission or absorption lines, we apply the continuum we measured via model 1 in fits to the rebinned data to the RGS1 and RGS2 spectra at full instrumental resolution. We selected model 1 instead of model 3 as we regard the MCD model to be more physical for BHCs than a simple blackbody model (the difference in the continuum shape from model three should be very small). In Figure 2, we plot the 90% confidence upper-limits on the strengths of emission or absorption features with widths less than or equivalent to the first-order RGS resolution. For visual clarity, we have rebinned the data in this plot by a factor of 10. It is clear from this plot that any narrow line features in the 0.6–2.3 keV range are very weak (equivalent width ~ 1 –5 eV for most of the bandpass) when GRS 1758–258 is in the off/soft state.

4. Discussion

Although we have observed the soft X-ray component in the off/soft state of GRS 1758–258, no clear emission or absorption features have been observed in the joint spectra of RGS1 and RGS2 (see Figures 1 and 2). Observations of BHCs 1E 1740.7–2942 (Cui et al. 2000) and SS 433 (Marshall et al. 2001) with *Chandra* have found evidence for extended regions around the X-ray sources which are too large to be an accretion disk but too small to be a supernova remnant. A central goal of our observation was to examine the nature of such an extended region in GRS 1758–258, if one exists. Since optically-thin, cooling plasmas produce strong line features, it is unlikely that the soft component we have measured is due to such a region. The improbable abundances required by fits with models for diffuse plasmas support this interpretation.

The jets from GRS 1758–258 observed in the radio band might be another potential source for X-ray line emission. Tentative evidence for lines from a jet are found in the *Chandra* observation of 1E 1740.7–2942 noted above; lines are clearly detected in the spectra of SS 433. The absence of lines that might be attributed to a jet in GRS 1758–258 is consistent with a picture in which jets are extinguished in the soft state in BHCs (Fender 2001). Recently, it has also been proposed that jets might produce the power-law component observed in BHCs (Markoff, Falcke, & Fender 2001). The observed absence of lines consistent with a jet, coupled with the diminished strength of the power-law component in the off/soft state, may support this model. Stronger conclusions must await the publication of radio data gathered during the off/soft state of GRS 1758–258.

The soft X-ray component we have measured is likely due primarily (but not necessarily entirely) to an accretion disk. We measure a disk temperature which is broadly consistent with results obtained with the *RXTE*/PCA by SHMS on 12–13 March 2001, and with a short soft state only five months previous to our observation (Goldwurm et al. 2001). From Table 1, it is clear that the temperature of the soft component and the 0.6–2.3 keV flux are dependent upon

the value of N_H which is used. Based on the results of SHMS, and our finding that a power-law component contributes less than 2% of the flux in the 0.6–2.3 keV range, it is possible that in the extended off/soft state the hard power-law flux merely turns-off and reveals the accretion disk.

The off/soft state is indicated by a steady decrease in the 3–25 keV flux from GRS 1758–258, and by a far softer spectrum than is observed when the source is in the more typical low/hard state (SHMS 2001). Such a decrease in flux is usually interpreted in terms of a decreasing \dot{m} . Advection-dominated accretion flow (ADAF) models adapted to BHCs (Esin, McClintock, & Narayan 1997; Esin et al. 1998) predict that a decrease in the mass accretion rate (\dot{m}) should be accompanied by spectral hardening. The spectral hardening may occur as the inner accretion disk is replaced by a hot, optically-thin region which may Comptonize seed photons and produce a power-law spectral component. In sharp contrast, the spectrum of GRS 1758–258 softens as the inferred \dot{m} decreases.

If the distance to a source and its inclination are known, the MCD model provides a measure of the temperature and inner radial extent of the accretion disk. In fact, the derived temperature and radius may be distorted by the Comptonization of disk photons by a coronal volume or a disk atmosphere. Shimura and Takahara (1995) have reported that a simple correction factor f_{col} can account for this effect; the effective disk temperature is given by $T_{eff} = T_{col}/f_{col}$, and the effective radius is given by $r_{eff} = f_{col}^2 r_{col}$. For BHCs, a typical value is $f_{col} = 1.7$ (see, e. g., Sobczak et al. 1999).

In Figure 3, we present constraints on the inner radial extent of the accretion disk. The best-fit color temperature and radius measured with MCD models in Table 1 are used. We assume a distance of 8.5 kpc to GRS 1758–258 based on its central Galactic position and column density. The inclination of GRS 1758–258 has not yet been measured, however the detection of jets in the radio band makes it unlikely that the system is seen face-on. We therefore assume an intermediate value for the inclination angle ($\theta_{incl} = 45^\circ$). We plot constraints on the inner radii calculated using no color correction ($f_{col} = 1.0$) and the typical value for BHCs ($f_{col} = 1.7$).

Given that the hard flux is diminished greatly in the off/soft state of GRS 1758–258, it is likely that the Comptonization of disk photons is not as strong an effect as in other BHCs and the color correction may not be required. If no color correction is applied, for reasonable values of the black hole mass in GRS 1758–258 the inner extent of the accretion disk is broadly consistent with the marginally stable circular orbit around a Schwarzschild black hole (see Figure 3). This finding may be inconsistent with ADAF models of other BHCs at relatively low implied values of \dot{m} (in some sources, however, X-ray flux and spectral states may be decoupled; see, e. g., Homan et al. 2001; Wijnands & Miller 2001). If the color correction is accurate, the inner disk extent is slightly recessed and consistent with ADAF models of Cygnus X-1 in the low/hard state ($r_{in} > 20 R_g$, Esin et al. 1998). However, the spectrum of Cygnus X-1 at lower implied values of \dot{m} is more consistent with an inner ADAF volume than the spectrum of GRS 1758–258. A simple ADAF interpretation might still be valid for this source if the soft component could be attributed to an extended cool

volume, but our results indicate that this is very unlikely. A model in which the inner advection region is peculiarly radiatively-inefficient might describe the off/soft state of GRS 1758–258.

Smith, Heindl, and Swank (Smith et al. 2001d) have discussed the long-term spectral variability of BHCs 1E 1740.7–2942, GRS 1758–258, GX 339–4, Cygnus X-1, and Cygnus X-3 in terms of two independent accretion flows. As SHMS note, the off/soft state is adequately described by this model. The possible cooling of the accretion disk which we measure supports this picture. It is interesting to note that Chen, Gehrels, and Leventhal (1994) have proposed that 1E 1740.7–2942 and GRS 1758–258 may accrete both through an accretion disk and via Bondi-Hoyle accretion from the relatively high-density ISM in the Galactic center. Observationally, the two-flow and disk-plus-Bondi-Hoyle accretion models may be very similar.

5. Acknowledgments

We wish to thank *XMM-Newton* PI Fred Jansen, and the *XMM-Newton* staff for executing this target-of-opportunity observation and their help in processing the data. RW was supported by NASA through Chandra fellowship grants PF9-10010, which is operated by the Smithsonian Astrophysical Observatory for NASA under contract NAS8–39073. BMG acknowledges the support of NASA through Hubble Fellowship grant HST-HF-01107.01-A awarded by the Space Telescope Science Institute, which is operated by the Association of Universities for Research in Astronomy, Inc., for NASA under contract NAS 5–26555. WHGL gratefully acknowledges support from NASA. This research has made use of the data and resources obtained through the HEASARC on-line service, provided by NASA-GSFC.

REFERENCES

- Arnaud, K., & Dorman, B., 2000, XSPEC is available via the HEASARC on-line service, provided by NASA-GSFC
- Bonnet-Buידaud, J. M., Haberl, F., Ferrando, P., Bennie, P. J., & Kendziorra, E., 2001, A & A, 365L, 282B
- Chen, W., Gehrels, N., & Leventhal, M., 1994, ApJ, 426, 586
- Cottam, J., Kahn, S. M., Brinkman, A. C., den Herder, J. W., & Erd, C., 2001, A & A, 365L, 277C
- Cui, W., et al., 2001, ApJ, 548, 394C
- Esin, A. A., McClintock, J. E., & Narayan, R., 1997, ApJ, 489, 865E
- Esin, A. A., Narayan, R., Cui, W., Grove, E. J., & Zhang, S., 1998, ApJ, 505, 854E
- Fender, R. P., 2001, MNRAS, 322, 31

- Gilfanov, M., et al., 1993, *ApJ*, 418, 844
- Goldwurm, A., Israel, D., Goldoni, P., Ferrando, P., Decourchelle, A., Mirabel, I. F., & Warwick, R. S., 2001, to appear in the Proc. of the Gamma-Ray Astrophysics 2001 Symposium, AIP, astro-ph/0106310
- Heindl, W. A., and Smith, D. M., 2001, to appear in “X-rays at Sharp Focus: Chandra Science Symposium ASP Conference Series”, 2002, eds. S. Vrtilek, E. M. Schlegel, and L. Kuhi, astro-ph/0107469
- Homan, J., et al., 2001, *ApJS*, 132, 377
- Markoff, S., Falcke, H., Fender, R., 2001, *A & A*, 372L, 25M
- Marshall, H. L., et al., 2001, *ApJ* subm.
- Mereghetti, S., 1994, *ApJ*, 433, L21
- Mereghetti, S., Cremonesi, D. I., Haardt, F., Murakami, T., Belloni, T., & Goldwurm, A., 1997, *ApJ*, 476, 829
- Mirabel, I. F., 1994, *ApJS*, 92, 369
- Mirabel, I. F., Rodriguez, L. F., Cordier, B., Paul, J., & Lebrun, F., 1992, *Nature*, 258, 215
- Mitsuda, K., et al., 1984, *PASJ*, 36, 741
- Rodriguez, L. F., Mirabel, I. F., & Marti, J., 1992, *ApJ*, 401, L15
- Sobczak, G. J., McClintock, J. E., Remillard, R. A., Bailyn, C. D., & Orosz, J. A., 1999, *ApJ*, 520, 776
- Shimura, T., and Takahara, F., 1995, *ApJ*, 445, 780S
- Smith, D. M., Markwardt, C. B., Heindl, W. A., & Swank, J. H., 2001a, *IAUC* 7595
- Smith, D. M., Heindl, W. A., Markwardt, C. B., & Swank, J. H., 2001b, *ATEL* 66
- Smith, D. M., Heindl, W. A., Markwardt, C. B., & Swank, J. H., 2001c, *ApJL*, in press, astro-ph/0103381
- Smith, D. M., Heindl, W. A., & Swank, J. H., 2001d, astro-ph/0103304
- Sunyaev, R., et al., 1991, *A & A*, 247, L29
- Tanaka, Y., and Lewin, W. H. G., 1995, in *X-ray binaries*, ed. W. H. G. Lewin, J. van Paradijs, & E. P. J. van den Heuvel (Cambridge: Cambridge Univ. Press), 126
- Wijnands, R., & Miller, J. M., 2001, *ApJL* subm., astro-ph/0105182

Table 1: Models and Results

Multicolor Disk Blackbody Fits							
Model	N_H (10^{22} cm^{-2})	kT (keV)	N_{MCD}	PL index	N_{PL} (10^{-3})	$L_{0.6-2.3}$ (10^{36} erg/s)	χ^2/dof
1	$2.28^{+0.07}_{-0.02}$	$0.34^{+0.01}_{-0.01}$	5850^{+1900}_{-1100}	2.75	<4.5	8^{+2}_{-2}	2030/1252
2	1.50	$0.60^{+0.01}_{-0.01}$	180^{+10}_{-10}	2.75	<0.6	$2.6^{+0.2}_{-0.2}$	2786/1251

Blackbody Fits							
Model	N_H (10^{22} cm^{-2})	kT (keV)	N_{BB} (E-3)	PL index	N_{PL} (10^{-3})	$L_{0.6-2.3}$ (10^{36} erg/s)	χ^2/dof
3	$2.09^{+0.06}_{-0.06}$	$0.286^{+0.007}_{-0.007}$	$9.1^{+0.9}_{-0.8}$	2.89	<5.1	$5.0^{+0.6}_{-0.4}$	1987/1252
4	1.50	$0.378^{+0.005}_{-0.004}$	$4.30^{+0.05}_{-0.05}$	2.89	<0.6	$2.37^{+0.03}_{-0.06}$	2361/1251
5	1.74	$0.332^{+0.002}_{-0.001}$	$5.66^{+0.08}_{-0.08}$	2.89	<1.6	$3.18^{+0.07}_{-0.04}$	2096/1251

Power-law Fits							
Model	N_H (10^{22} cm^{-2})	–	–	PL index	N_{PL}	$L_{0.6-2.3}$ (10^{36} erg/s)	χ^2/dof
6	$2.9^{+0.1}_{-0.1}$	–	–	$5.2^{+0.2}_{-0.2}$	$2.2^{+0.4}_{-0.4}$	48^{+9}_{-8}	2222/1251

Note. — Results of fitting the background-subtracted, rebinned first-order RGS1 and RGS2 spectra jointly with standard models, in the 0.6–2.3 keV bandpass (90% confidence errors). The power-law indices in models 1–5 are fixed to the values obtained by Smith et al. (2001) using *RXTE* within the off/soft state as this component cannot be constrained in the limited energy range of the RGS. The power-law component is not required in fits 1–5 and the quoted normalizations and fluxes are upper-limits (90% conf.). The neutral hydrogen column density, N_H , is allowed to float in models 1, 3, and 6. In models 2 and 5, N_H is fixed to the values reported by Smith et al. (2001) to allow for more direct comparison to those results. Similarly, N_H is fixed to the value reported by Goldwurm et al. (2001) in fits to *XMM-Newton* EPIC-MOS data obtained in September, 2000. Model 6 is a simple power-law; the obtained χ^2 statistic is slightly worse than the models dominated by thermal components, but the measured index is very different than those reported in other BHCs (see, e. g., Tanaka & Lewin 1995). In fits 1–5, the power-law contribution to the 0.6–2.3 keV luminosity is <2% of the total; luminosities are calculated assuming a distance of 8.5 kpc. Luminosities quoted above are “unabsorbed” luminosities.

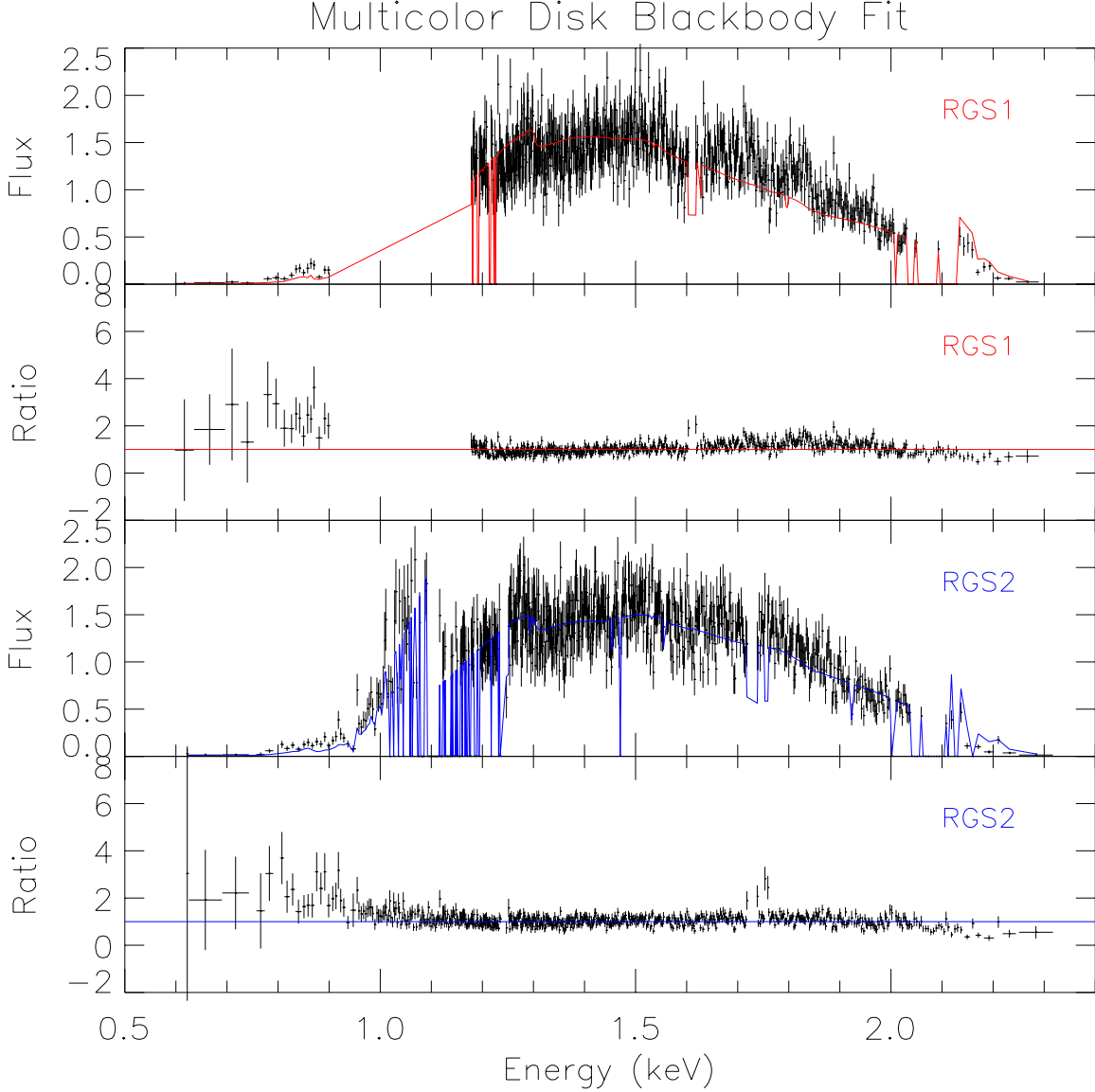


Fig. 1.— Results of fitting to RGS1 and RGS2 jointly with a model consisting of multicolor disk blackbody and power-law components. The flux (in units of normalized counts/cm²/s) and data/model ratio are shown; at top: RGS1, at bottom: RGS2. Fits with a model consisting of simple blackbody and power-law components, and of only a power-law component (see Table 1) yield similar results in terms of the fit and data/model ratio. The large gap seen in RGS1 (0.9–1.2 keV) is due to a failed CCD in that region of the dispersed spectrum. Points where the model goes through flux bins consistent with zero (in RGS1: near 1.2 keV, and 2.0–2.1 keV; in RGS2: between 1.0–1.3 keV, and 2.0–2.1 keV) are an artifact of our rebinning (requirement of 20 counts per channel) in regions of low or rapidly changing effective area.

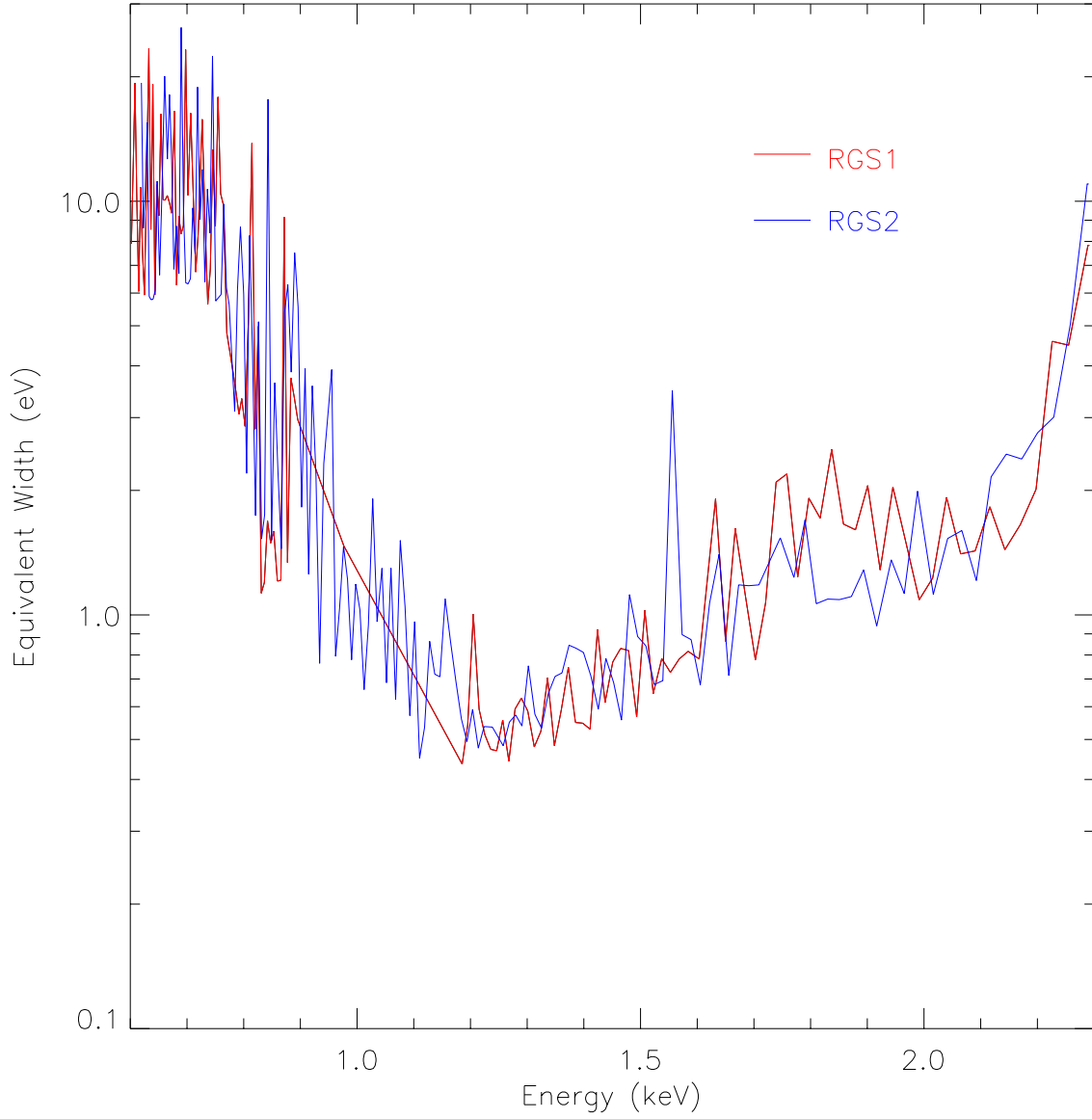


Fig. 2.— Upper limits (90% confidence) on the strength of narrow, single-bin emission or absorption features in the RGS spectrum of GRS 1758–258. RGS1 is shown in red, and RGS2 is shown in blue. The limits have been rebinned by a factor of 10 for visual clarity. These limits are based on our best fit to the continuum with the MCD multicolor disk blackbody model; results from a simple black body continuum model are very similar.

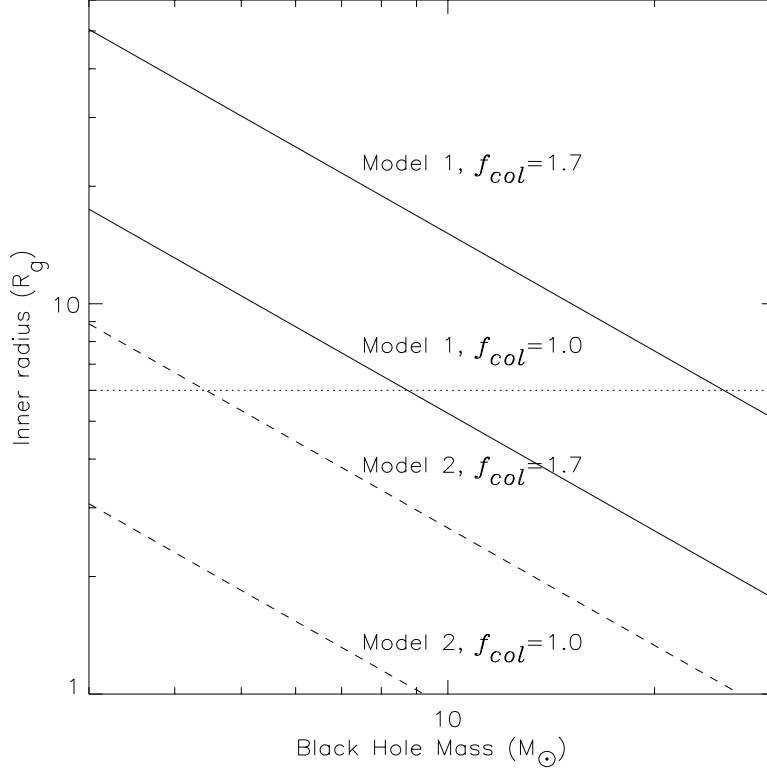


Fig. 3.— Inner accretion disk radii derived via the multicolor disk blackbody model, assuming an intermediate inclination ($\theta_{\text{incl}} = 45^\circ$) and a distance of 8.5 kpc. Fits with model 1 (N_H free) yield inner radii of 77 km and 220 km, for $f_{col} = 1.0$ and $f_{col} = 1.7$, respectively. Fits with model 2 (N_H fixed) yield inner radii of 14 km and 39 km, for $f_{col} = 1.0$ and $f_{col} = 1.7$, respectively. The marginally stable circular orbit around a Schwarzschild black hole is $6 R_g$; this radius is indicated with a dotted line.